Anomalies in isothermal compressibility and exponent of pressure in spin-orbit-coupled degenerate Fermi gases

Chenggong Liang,[1,2] Yuexin Huang,[2] Feihong Liu,[2] Yunbo Zhang,[1,*] Guangcan Guo,[2,3,4] and Ming Gong[2,3,4,†]

[1]*Institute of Theoretical Physics, Shanxi University, Taiyuan, Shanxi 030006, China*

[2]*CAS Key Laboratory of Quantum Information, University of Science and Technology of China, Hefei 230026, China*

[3]*Synergetic Innovation Center of Quantum Information and Quantum Physics, University of Science and Technology of China, Hefei 230026, China*

[4]*CAS Center For Excellence in Quantum Information and Quantum Physics, University of Science and Technology of China, Hefei 230026, China*

(Received 10 September 2018; accepted 7 July 2020; published 30 July 2020)

The spin-orbit coupling (SOC) in degenerate Fermi gases can fundamentally change the fate of s-wave superfluids. Here we report the anomalous isothermal compressibility κ_T in the degenerate Fermi gases with both SOC and Zeeman field. Starting from the Gibbs-Duhem equation, we show that κ_T comes from both the explicit contribution of chemical potential and the implicit contribution of the order parameter. In the Bardeen-Cooper-Schrieffer (BCS) limit, κ_T is determined by the explicit compressibility, which is proportional to the density of states at the Fermi surface; while in the Bose-Einstein condensate (BEC) regime it is determined by the implicit compressibility, which is uniquely given by the scattering length. Between these two limits, we find a pronouncedly enhanced compressibility in the gapless Weyl phase regime, which is attributed to a remanent effect of the instability of degenerate Fermi gases towards phase separation. This enhanced compressibility also leads to an anomaly in the exponent of pressure. A connection between this exponent and the polytropic index is established. These predictions can be measured from the anomaly in sound velocity, density fluctuation, and collective vibration frequencies.

DOI: 10.1103/PhysRevA.102.013327

Spin-orbit coupling (SOC) can modify the single-particle band structures [1] and thus influences the fate of degenerate gases. In bosonic gases, the ground state may carry a finite momentum [2–4] in either the plane-wave phase or the stripe phase, depending on the two-body scattering lengths [5–10]. The transition between these two phases is described by a Dicke model [11–13]. Recently, this system has been used to search for supersolid phases [14–16]. It can also be used to study the scaling law of defects by the Kibble-Zurek mechanism during quench dynamics [17,18]. In Fermi gases, the physics is different. This interaction can make the spin polarization momentum dependent, thus when an energy gap is opened by a perpendicular Zeeman field, effective p-wave pairing is allowed in the same band with only s-wave interaction. This mechanism has stimulated great effort in experiments for topological superconducting phases and Majorana zero modes [19–26]. Furthermore, this interaction can lead to various topological superfluids [27–35]. In the case of inversion-symmetry breaking, this system can support superfluids with finite-momentum pairing [36–42]. While these superfluids have been widely explored in the literature, their thermodynamic properties are not yet well understood.

In this work, we focus on the effect of SOC and the Zeeman field on the isothermal compressibility (IC), which measures the change of volume as a response to pressure [43,44],

$$\kappa_T = -\frac{1}{V}\left(\frac{\partial V}{\partial P}\right)_{T,N}. \tag{1}$$

Here the thermodynamic variables P, V, T, and N correspond to pressure, volume, temperature, and total number of particles, respectively. For an ideal gas described by the Clapeyron equation, $\kappa_T = 1/P$; while in solid materials, $\kappa_T = 1/B$, with B being the Young's modulus [45]. In the ideal gas, this quantity is related to sound velocity via the Newton-Laplace formula $c_s = \sqrt{\gamma V/N\kappa_T}$, where γ is the heat capacity ratio [46]. From this definition, we see that the more compressible the system is, the larger this value will be. For this reason, it can be used to identify the boundaries between superfluids and insulators [47–51] and between normal phase and Bose-Einstein condensate (BEC). In a BEC, κ_T will diverge since the zero-momentum condensate does not contribute to pressure [43,44,52]. In experiments, κ_T has been measured with both fermions [51,53,54] and bosons [55–57].

In this work, we show that κ_T comes from the explicit contribution of the chemical potential and the implicit contribution of the order parameter. In the Bardeen-Cooper-Schrieffer (BCS) limit with vanished pairing strength, κ_T is determined by the density of states at the Fermi surface from the explicit compressibility, while in the BEC limit, it is determined by the scattering length from the implicit compressibility. Between

*ybzhang@sxu.edu.cn
†gongm@ustc.edu.cn

these two limits, we find a pronouncedly enhanced IC in the Weyl superfluid with two Weyl points, which is attributed to a remanent effect of the instability of degenerate Fermi gases from phase separation (PS). This anomaly also leads to anomalous behavior in the exponent of pressure. These predictions can be measured from sound velocity, density fluctuation, and collective vibration frequencies.

We start from the Gibbs-Duhem equation [43,44] $-SdT + VdP = \sum_\sigma N_\sigma d\mu_\sigma$, where $\mu_\uparrow = \mu + h_z$, $\mu_\downarrow = \mu - h_z$, μ is the chemical potential, h_z is the effective Zeeman field, S is the total entropy, $\sigma = \uparrow, \downarrow$, and $N = \sum_\sigma N_\sigma$ is the total number of particles. For fixed T, it establishes a direct relation between pressure and particle densities via $P = P(T, n_\uparrow, n_\downarrow)$, with $n_\sigma = N_\sigma/V$. Then,

$$\frac{1}{\kappa_T} = -\left[V\left(\frac{\partial P}{\partial n_\uparrow}\right)_{T,n_\downarrow}\left(\frac{\partial n_\uparrow}{\partial V}\right)_{T,n_\downarrow} + (\uparrow\leftrightarrow\downarrow)\right]. \quad (2)$$

Using $\frac{\partial n_\sigma}{\partial V} = -N_\sigma/V$ and the Maxwell relation $\frac{\partial P}{\partial N_\sigma} = -\frac{\partial \mu_\sigma}{\partial V}$, we have

$$\frac{1}{\kappa_T} = -\sum_\sigma N_\sigma\left(\frac{\partial \mu_\sigma}{\partial V}\right)_T = \sum_{\sigma\sigma'\in\uparrow,\downarrow}\frac{1}{\kappa_{\sigma\sigma'}}, \quad (3)$$

where $\kappa^{-1}_{\sigma\sigma'} = n_\sigma n_{\sigma'}\frac{\partial \mu_\sigma}{\partial n'_\sigma}$. This result is true for a system with arbitrary number of components. In the limiting case that n_σ is independent of $\mu_{\sigma'}$ for $\sigma \neq \sigma'$, one finds $\kappa^{-1}_{\sigma\sigma'} = 0$. Otherwise, $\kappa^{-1}_{\sigma\sigma'} \neq 0$, thus Eq. (3) is always well defined. Moreover, in the limit with $\mu_\sigma = \mu$, it is reduced to $\kappa_T = \frac{1}{n^2}(\frac{\partial n}{\partial \mu})_T$, which was used in the literature [47–51]. By definition, $\kappa_T \neq 0$ even at zero temperature.

We employ this framework to study the IC in degenerate Fermi gases with SOC and Zeeman field. The single-particle Hamiltonian reads $H_0 = \sum_{\mathbf{k}\sigma\sigma'} c^\dagger_{\mathbf{k}\sigma}[\xi_{\mathbf{k}} + \alpha(k_y\sigma_x - k_x\sigma_y) + h_z\sigma_z]_{\sigma\sigma'}c_{\mathbf{k}\sigma'}$, where $\xi_{\mathbf{k}} = \frac{k^2}{2m} - \mu$, $\mathbf{k} = (k_x, k_y, k_z)$, α is the SOC coefficient and $\sigma_{x,y,z}$ are Pauli matrices, assuming $\hbar = 1$. In the presence of s-wave interactions, one can define a uniform pairing order $\Delta = \frac{g}{V}\sum_{\mathbf{k}}\langle c_{-\mathbf{k}\uparrow}c_{\mathbf{k}\downarrow}\rangle$, where g is the interaction strength. Let us define the thermodynamic potential Ω through $Z = e^{-\beta\Omega} = \mathrm{Tr}(e^{-\beta H})$, with $\beta = 1/k_BT$ and $PV = -\Omega$, then

$$\Omega = \sum_{\mathbf{k}}\xi_k - \frac{1}{\beta}\sum_{\mathbf{k}\lambda}\ln\left[2\cosh\left(\beta E^\lambda_{\mathbf{k}}/2\right)\right] - \frac{V|\Delta|^2}{g}, \quad (4)$$

where $E^\lambda_{\mathbf{k}} = (|\gamma_{\mathbf{k}}|^2 + \xi^2_{\mathbf{k}} + h_z^2 + |\Delta|^2 + 2\lambda E_0)^{1/2}$, $E_0 = [h_z^2(\xi^2_{\mathbf{k}} + |\Delta|^2) + |\gamma_{\mathbf{k}}|^2\xi^2_{\mathbf{k}}]^{1/2}$, $|\gamma_{\mathbf{k}}|^2 = \alpha^2(k_x^2 + k_y^2)$ and $\lambda = \pm 1$. The values of μ and Δ are determined by $n_\sigma = -\frac{1}{V}\frac{\partial\Omega}{\partial\mu_\sigma}$ and $\frac{\partial\Omega}{\partial\Delta} = 0$, in which the divergence of Ω is regularized by $\frac{1}{g} = \frac{m}{4\pi a_s} - \frac{1}{V}\sum_{\mathbf{k}}\frac{1}{k^2/m}$, with a_s being the scattering length [27].

Notice that Δ is also an implicit function of μ, thus to compute κ_T, we may take the derivative of the density with respect to μ explicitly (e) and implicitly (i) through Δ as [58]

$$\left(\frac{\partial n_\sigma}{\partial \mu_{\sigma'}}\right)_T = \left(\frac{\partial n_\sigma}{\partial \mu_{\sigma'}}\right)_{T,i} + \left(\frac{\partial n_\sigma}{\partial \mu_{\sigma'}}\right)_{T,e}, \quad (5)$$

where $(\frac{\partial n_\sigma}{\partial \mu_{\sigma'}})_{T,i} = -(\frac{\partial^2\Omega}{\partial\mu^2})_{T,\Delta}$. The implicit term can be written as $(\frac{\partial n_\sigma}{\partial \mu_{\sigma'}})_{T,i} = (\frac{\partial n_\sigma}{\partial\Delta})_{T,\mu}(\frac{\partial\Delta}{\partial\mu_{\sigma'}})_{T,i}$. With the aid of $\frac{\partial\Omega}{\partial\Delta} = 0$, we find $(\frac{\partial\Delta}{\partial\mu})_{T,i} = -(\frac{\partial^2\Omega}{\partial\mu\partial\Delta}/\frac{\partial^2\Omega}{\partial^2\Delta})$, thus $(\frac{\partial n}{\partial\mu})_{T,i} = (\frac{\partial^2\Omega}{\partial\Delta\partial\mu})^2/\frac{\partial^2\Omega}{\partial\Delta^2}$. Collecting these results yield

$$\kappa_T = \kappa_{T,e} + \kappa_{T,i}, \quad (6)$$

where their expressions are presented below:

$$\kappa_{T,e} = \frac{\sum_{\mathbf{k},\lambda}\left(Y^\lambda_{\mathbf{k}} - X^\lambda_{\mathbf{k}}\right)\left(\frac{\xi_{\mathbf{k}}Q^\lambda_{\mathbf{k}}}{E^\lambda_{\mathbf{k}}}\right)^2 + X^\lambda_{\mathbf{k}}\left(Q^\lambda_{\mathbf{k}} - \lambda\frac{\xi^2_{\mathbf{k}}P^2_{\mathbf{k}}}{E^3_0}\right)}{2n^2}, \quad (7)$$

and

$$\kappa_{T,i} = \frac{\left\{\sum_{\mathbf{k},\lambda}\xi_{\mathbf{k}}\left[\left(X^\lambda_{\mathbf{k}} - Y^\lambda_{\mathbf{k}}\right)\frac{Q^\lambda_{\mathbf{k}}S^\lambda_{\mathbf{k}}}{E^{\lambda\,2}_{\mathbf{k}}} + \lambda X^\lambda_{\mathbf{k}}\frac{h_z^2P_{\mathbf{k}}}{E^3_0}\right]\right\}^2}{2n^2\sum_{\mathbf{k},\lambda}\left[\left(X^\lambda_{\mathbf{k}} - Y^\lambda_{\mathbf{k}}\right)\left(\frac{S^\lambda_{\mathbf{k}}}{E^\lambda_{\mathbf{k}}}\right)^2 - \lambda X^\lambda_{\mathbf{k}}\frac{h_z^4}{E^3_0}\right]}. \quad (8)$$

Here $X^\lambda_{\mathbf{k}} = \tanh(\frac{\beta E^\lambda_{\mathbf{k}}}{2})/E^\lambda_{\mathbf{k}}$, $Y^\lambda_{\mathbf{k}} = \beta[1 - \tanh^2(\frac{\beta E^\lambda_{\mathbf{k}}}{2})]/2$, $P_{\mathbf{k}} = h_z^2 + |\gamma_{\mathbf{k}}|^2$, $Q^\lambda_{\mathbf{k}} = 1 + \lambda P_{\mathbf{k}}/E_0$, and $S^\lambda_{\mathbf{k}} = 1 + \lambda h_z^2/E_0$.

Equations (7) and (8) are two major expressions derived in this work. To illustrate their physical significance, let us discuss their exact results from several solvable limits:

(I) Without many-body interactions, $\kappa_{T,i} = 0$, since $\Delta = 0$. The density is determined as $n = \frac{1}{V}\sum_{\mathbf{k}\lambda} n_{\mathbf{k}\lambda}$, and the total compressibility $\kappa_T = \frac{\beta}{4n^2V}\sum_{\mathbf{k}\lambda}[1 - \tanh^2(\beta E_{\mathbf{k}\lambda}/2)]$. Obviously when $T = 0$, $\kappa_T = \frac{1}{2n^2V}\rho(\mu)$, where $\rho(\mu) \propto \sqrt{\mu}$ is the density of states at the Fermi surface. As a consequence, we see that, in the metallic phases with $\rho(\mu) \neq 0$, $\kappa_T \neq 0$; while in the insulator phases with $\rho(\mu) = 0$, $\kappa_T = 0$, for which reason this quantity can be used to identify the boundaries of the Mott insulator and supersolid phases [47–51].

(II) Without SOC and the Zeeman field, these compressibilities can be solved analytically. In this case, $E^\lambda_{\mathbf{k}} = E_{\mathbf{k}}$, then $\kappa_{T,i} = \frac{1}{n^2V}(\sum_{\mathbf{k}}\xi_{\mathbf{k}}/E^3_{\mathbf{k}})^2/(\sum_{\mathbf{k}}1/E^3_{\mathbf{k}})$, and $\kappa_{T,e} = \frac{1}{n^2V}\sum_{\mathbf{k}}(1/E_{\mathbf{k}} - \xi^2_{\mathbf{k}}/E^3_{\mathbf{k}})$, where $E_{\mathbf{k}} = (\xi^2_{\mathbf{k}} + |\Delta|^2)^{1/2}$. Let us define the two integrals

$$I_1 = \frac{1}{V}\sum_{\mathbf{k}}\frac{\xi_{\mathbf{k}}}{E^3_{\mathbf{k}}} = \frac{m^{3/2}K(x)}{\sqrt{2}\pi^2\varepsilon_g^{1/2}}, \quad x = \frac{1}{2}\left(1 + \frac{\mu}{\varepsilon_g}\right), \quad (9)$$

$$I_2 = \frac{1}{V}\sum_{\mathbf{k}}\frac{1}{E^3_{\mathbf{k}}} = m^{3/2}\frac{2\varepsilon_g E(x) + (\mu - \varepsilon_g)K(x)}{\sqrt{2}\pi^2\Delta^2\varepsilon_g^{1/2}}, \quad (10)$$

where $\varepsilon_g = (\mu^2 + \Delta^2)^{1/2}$, $E(x)$ is the complete elliptic integral, and $K(x)$ is the complete elliptic integral of the first kind. The two compressibilities can be written as $\kappa_{T,i} = I_1^2/(I_2n^2)$ and $\kappa_{T,e} = \Delta^2 I_2/n^2$. In the BCS limit, $\Delta \to 0$ and μ approaches the Fermi energy. In the BEC limit [59],

$$\Delta = \frac{2\sqrt{n\pi}}{\sqrt{a_s}m}, \quad \mu = \frac{\epsilon_b}{2} + \frac{a_s n\pi}{m}, \quad (11)$$

where the molecular binding energy $\epsilon_b = -(ma_s^2)^{-1}$. We see that, in the BCS limit, $\kappa_{T,i} \to 0$ and $\kappa_{T,e} \to \sqrt{2}m^{3/2}\sqrt{\mu}/(\pi^2n^2)$, while in the BEC limit, $\kappa_{T,e} \to 0$ and $\kappa_{T,i} \to \sqrt{2}m^{3/2}(-\mu)^{1/2}/(\pi n^2)$. In the latter limit, μ plays the role of binding energy, which is *almost* independent of particle density n, thus it does not make a significant contribution to IC. In this regime we have $\kappa_T \propto 1/k_Fa_s$. It is also interesting to find that the ratio of these two compressibilities in the whole parameter regime can be written in a universal form

$$\frac{\kappa_{T,i}}{\kappa_{T,e}} = \left(\frac{K(x)\Delta}{2\varepsilon_g E(x) + (\mu - \epsilon_g)K(x)}\right)^2, \quad (12)$$

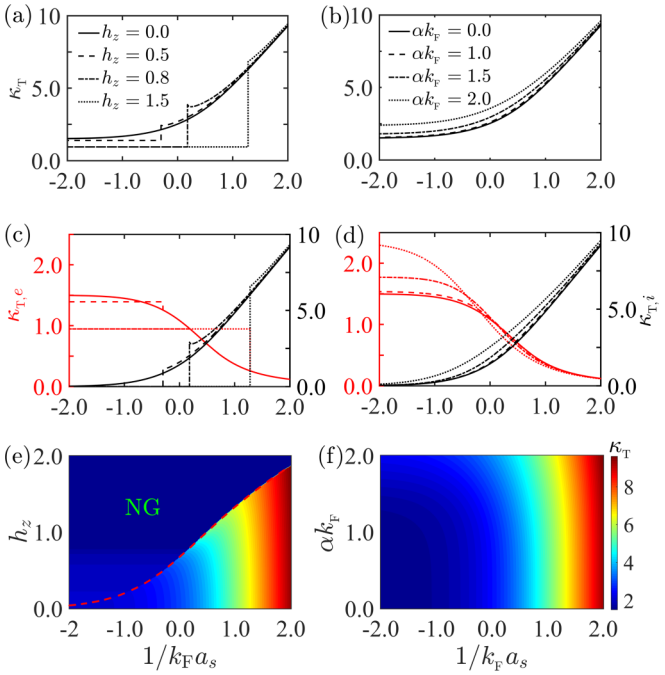

FIG. 1. (a), (b) IC with only Zeeman field (left column) and SOC (right column). (c), (d) The two compressibilities $\kappa_{T,e}$ and $\kappa_{T,i}$ for these two cases. (e), (f) Contour plot of IC as a function of Zeeman field (SOC) and scattering length. In a NG, $\Delta = 0$.

which depends only on the ratio of Δ and μ, following Eqs. (9) and (10).

These two compressibilities [Eqs. (7) and (8)] can be reduced to the results with only SOC in Ref. [60] by letting $h_z = 0$. The interesting point is that, in the presence of both SOC and the Zeeman field, the excitation spectra may become gapless in the Weyl superfluids, in which the compressibilities may no longer be always larger than zero, giving rise to instability towards the PS phase. In the following discussion, we utilize this feature.

Next, we determine the value of μ and Δ self-consistently at zero temperature [61,62]. The Fermi momentum $k_F = (3\pi^2 n)^{1/3}$ and Fermi energy $\epsilon_F = k_F^2/(2m)$ serve as basic scales for momentum and energy, respectively. The pressure will be presented in units of $n\epsilon_F$, so κ is expressed in units of $\kappa_0 = 1/(n\epsilon_F)$ [63]. We first discuss the role of SOC and the Zeeman field in Fig. 1. In the BCS limit, the pairing is destroyed when $|h_z| > |\Delta|$, giving rise to the normal gas (NG) phase. In the BCS limit with only the Zeeman field, we find that, when $h_z = 0$, $\kappa_T = 1.5$, while in the fully spin-polarized phase ($h_z \geqslant 0.8$), $\kappa_T = 0.945$. The ratio between them coincides with the theoretical value of $2^{2/3}$. These results demonstrate the opposite roles played by SOC and the Zeeman field; that is, $\rho(\mu)$ is reduced by the Zeeman field but enhanced by SOC. In the BEC limit, $\kappa_T \propto 1/k_F a_s$. These limits are fully consistent with the results in (I) and (II).

The physics is completely changed in the presence of both terms; see Fig. 2. We find a significantly enhanced IC, by about one order of magnitude, in some proper parameter regimes. This enhanced compressibility is more likely to be found in the regime with a relatively large Zeeman field and weak SOC. Especially, we find that the peak position depends

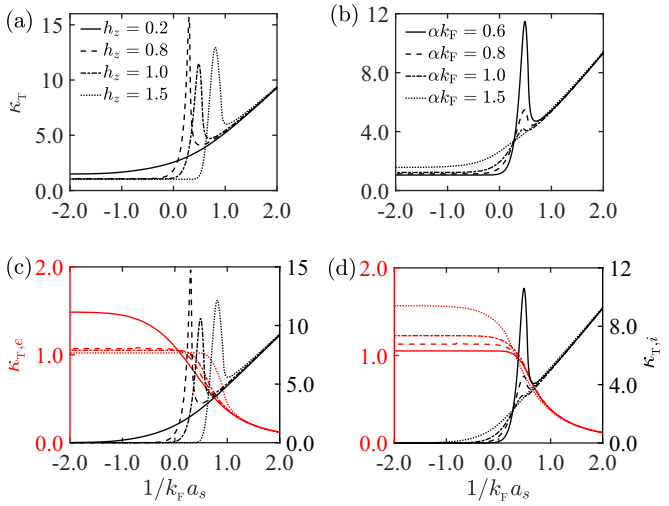

FIG. 2. (a), (b) IC with both Zeeman field and SOC. (c), (d) Corresponding explicit and implicit compressibilities. The other parameter in panels (a) and (c) is $\alpha k_F = 0.6$; while in panels (b) and (d) it is $h_z = 1.0$.

more strongly on the Zeeman field. In Figs. 2(c) and 2(d), we find that this peak arises from the implicit compressibility, while the explicit one is always a smooth function of $1/k_F a_s$. To further determine the reason for this anomaly, we plot the numerator and denominator of $\kappa_{T,i}$ in Fig. 3. It should be noticed that Δ is determined by the global minima of Ω, thus the denominator given by $\partial^2\Omega/\partial\Delta^2$ is related to the stability of this global minima, which is unstable when $\partial^2\Omega/\partial\Delta^2 < 0$. The local minima in the denominator accounts for the anomalous compressibility, which is more likely to be found in the gapless phase [31,64,65]. We illustrate this physics in Figs. 4(a) and 4(b) by plotting the excitation spectra for the peaks in Figs. 2(a) and 2(b) for the superfluid with two Weyl points. By increasing of the scattering length, the Weyl points

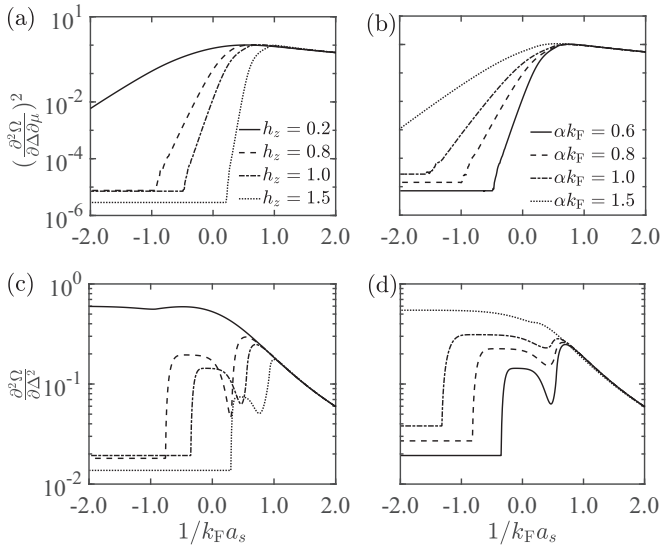

FIG. 3. The numerator and denominator of the implicit compressibility $\kappa_{T,i}$ as a function of scattering length with different Zeeman fields and SOC strengths. When $\Delta = 0$, $\kappa_{T,i} = 0$ accounts for the plateau in the BCS limit.

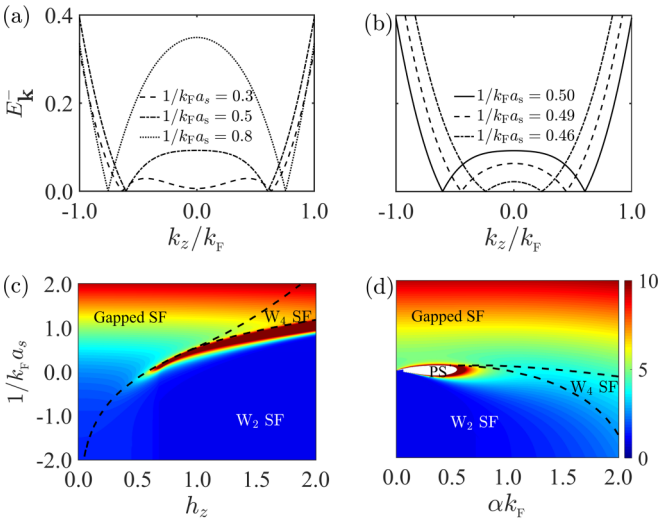

FIG. 4. (a), (b) Excitation spectra of $E_{\mathbf{k}-}$ for the three IC peaks in Figs. 2(a) and 2(b), respectively, with $k_x = k_y = 0$. The gapless points can only happen on the k_z axis, in which the solutions of $E_{\mathbf{k}-} = 0$ mark the Weyl points [27]. In panel (a) we have used $\alpha k_F = 0.6$ and in panel (b) $h_z = 1.0$. (c), (d) Phase diagram and contour plot of the IC. The white regime in panel (d) corresponds to the unstable PS phase identified by $\kappa_T < 0$. In each figure, $W_{2/4}$ SF denotes topological Weyl superfluids with two and four Weyl points, respectively.

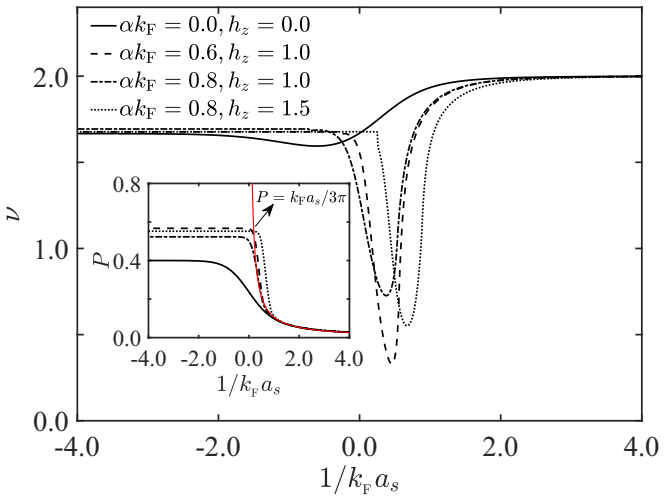

FIG. 5. Exponent of pressure ν in degenerate Fermi gases with SOC and Zeeman field. The two limits with $\nu = 5/3$ (BCS limit) and $\nu = 2$ (BEC limit) have been determined exactly in the main text. Inset shows the corresponding evolution of pressure P, which in the BEC limit can be obtained exactly as $P = k_F a_s/(3\pi)$ in units of $1/\kappa_0 = n\epsilon_F$.

are destroyed and the superfluid enters the trivial gapped phase, in which the compressibility becomes extremely large due to the condensate of molecules at zero momentum.

We plot the phase diagram and the contour plot of IC in Figs. 4(c) and 4(d). The phase diagram is classified according to the number of Weyl points in momentum space [27]. There is a small regime for PS determined by $\kappa_T < 0$ from $\partial^2\Omega/\partial\Delta^2 < 0$, in which the thermodynamic potential Ω exhibits two local minima in space by μ and Δ [31,64,65]. This instability is suppressed by SOC due to the effective p-wave pairing. We find that the enhanced IC in Fig. 4(c) happens near the boundary between the two Weyl superfluids, with the corresponding peak position depending strongly on the Zeeman field. We attribute this anomaly as a remanent effect of the instability of the gapless superfluids. We emphasize that, across the boundary of topological phase transition, the compressibility is not necessarily anomalous since it is not directly related to gap closing and reopening [66].

Finally, we address the fundamental consequence of this anomalous compressibility in its measurement. We come back to the original definition in Eq. (1) by assuming an infinitesimal change of system size via $L' = e^{\eta}L = (1+\eta)L$, then $dV = D\eta V$, where D is the dimension of the system. The corresponding pressure can be written as $P' = e^{-\eta D\nu}P = (1-\eta D\nu)P$, where ν defines the exponent of pressure. Then we have

$$\nu = 1/(\kappa_T P). \tag{13}$$

When the relation between P and V (or μ and n) can be written in the form of polytropic equation $PV^{\tilde{\gamma}} = C$ (or equivalently $\mu \propto n^{\tilde{\gamma}}$ [67,68]), then $\nu = \tilde{\gamma}$. For the ideal Fermi gases in the BCS limit, $\nu = 5/3$; while in the BEC limit with free Bose gases, $P = k_F a_s/3\pi$ in units of $1/\kappa_0$ [from Eq. (11)], we have $\nu = 2$. The numerical result for this exponent is shown in Fig. 5, which exhibits a strong minimum near the BEC-BCS crossover regime arising mainly from the anomaly of compressibility κ_T. The position of this minima and its amplitude depend strongly on the Zeeman field and SOC strengths. We emphasize that, without SOC and the Zeeman field, ν agrees with the polytropic index in the BEC, BCS and unitary limits with $\tilde{\gamma} = 2$, $5/3$, and $5/3$, respectively [69]. In experiments, this exponent can be directly measured from the vibration frequencies in a slowly rotating trap [67–72]. It may also be revealed from the particle density fluctuation since $\langle \delta n^2 \rangle \sim \kappa_T k_B T$ [43,44].

To conclude, we report some anomalous behavior in degenerate Fermi gases with SOC and the Zeeman field. The IC is shown to have a simple interpretation in the BCS and BEC limits. In the BCS limit it is proportional to density of states at the Fermi surface, while in the BEC limit it is proportional to $1/a_s$. Between these two limits, anomaly in IC can be observed as a remanent effect of instability towards PS, which also leads to anomaly in the exponent of pressure. These results pave the way for exploring other thermodynamic properties in the degenerate Fermi gases, including the superfluids with finite-momentum pairing [73]. In experiments, these predictions can be measured from the sound velocity, the density fluctuation, and the collective vibration frequencies.

The authors thank H. G. Luo and Zhen Zheng for valuable discussion. This work is supported by the National Natural Science Foundation (NSFC) under Grants No. 11774328, No. 11674201, and No. 11474189 and the National Key Research and Development Program of China (Grants No. 2016YFA0301700 and No. 2017YFA0304504). M.G. is also supported by the USTC start-up funding.

[1] J. Sinova, D. Culcer, Q. Niu, N. A. Sinitsyn, T. Jungwirth, and A. H. MacDonald, Universal Intrinsic Spin Hall Effect, Phys. Rev. Lett. **92**, 126603 (2004).

[2] Y.-J. Lin, K. Jimenez-Garcia, and I. B. Spielman, Spin–orbit-coupled Bose–Einstein condensates, Nature (London) **471**, 83 (2011).

[3] V. Galitski and I. B. Spielman, Spin-orbit coupling in quantum gases, Nature (London) **494**, 49 (2013).

[4] B. K. Stuhl, H.-I. Lu, L. M. Aycock, D. Genkina, and I. B. Spielman, Visualizing edge states with an atomic Bose gas in the quantum Hall regime, Science **349**, 1514 (2015).

[5] C. Wang, C. Gao, C.-M. Jian, and H. Zhai, Spin-Orbit Coupled Spinor Bose-Einstein Condensates, Phys. Rev. Lett. **105**, 160403 (2010).

[6] T. Ozawa and G. Baym, Ground-state phases of ultracold bosons with Rashba-Dresselhaus spin-orbit coupling, Phys. Rev. A **85**, 013612 (2012).

[7] T. Ozawa and G. Baym, Stability of Ultracold Atomic Bose Condensates with Rashba Spin-Orbit Coupling against Quantum and Thermal Fluctuations, Phys. Rev. Lett. **109**, 025301 (2012).

[8] J.-M. Cheng, X.-F. Zhou, Z.-W. Zhou, G.-C. Guo, and M. Gong, Symmetry-enriched Bose-Einstein condensates in a spin-orbit-coupled bilayer system, Phys. Rev. A **97**, 013625 (2018).

[9] Q. Sun, L. Wen, W.-M. Liu, G. Juzeliūnas, and A.-C. Ji, Tunneling-assisted spin-orbit coupling in bilayer Bose-Einstein condensates, Phys. Rev. A **91**, 033619 (2015).

[10] T.-L. Ho and S. Zhang, Bose-Einstein Condensates with Spin-Orbit Interaction, Phys. Rev. Lett. **107**, 150403 (2011).

[11] C. Hamner, C. Qu, Y. Zhang, J. J. Chang, M. Gong, C. Zhang, and P. Engels, Dicke-type phase transition in a spin-orbit-coupled Bose–Einstein condensate, Nat. Commun. **5**, 4023 (2014).

[12] Y. Zhang, G. Chen, and C. Zhang, Tunable spin-orbit coupling and quantum phase transition in a trapped Bose-Einstein condensate, Sci. Rep. **3**, 1937 (2013).

[13] R. H. Dicke, Coherence in spontaneous radiation processes, Phys. Rev. **93**, 99 (1954).

[14] J. Léonard, A. Morales, P. Zupancic, T. Esslinger, and T. Donner, Supersolid formation in a quantum gas breaking a continuous translational symmetry, Nature (London) **543**, 87 (2017).

[15] J.-R. Li, J. Lee, W. Huang, S. Burchesky, B. Shteynas, F. Ç. Top, A. O. Jamison, and W. Ketterle, A stripe phase with supersolid properties in spin–orbit-coupled Bose–Einstein condensates, Nature (London) **543**, 91 (2017).

[16] R. Liao, Searching for Supersolidity in Ultracold Atomic Bose Condensates with Rashba Spin-Orbit Coupling, Phys. Rev. Lett. **120**, 140403 (2018).

[17] S. Wu, Y. Ke, J. Huang, C. Lee, *et al.*, Kibble-Zurek scalings of continuous magnetic phase transitions in spin-1 spin-orbit-coupled Bose-Einstein condensates, Phys. Rev. A **95**, 063606 (2017).

[18] W. H. Zurek, U. Dorner, and P. Zoller, Dynamics of a Quantum Phase Transition, Phys. Rev. Lett. **95**, 105701 (2005).

[19] V. Mourik, K. Zuo, S. M. Frolov, S. R. Plissard, E. P. A. M. Bakkers, and L. P. Kouwenhoven, Signatures of Majorana fermions in hybrid superconductor-semiconductor nanowire devices, Science **336**, 1003 (2012).

[20] M. T. Deng, C. L. Yu, G. Y. Huang, M. Larsson, P. Caroff, and H. Q. Xu, Anomalous zero-bias conductance peak in a Nb-InSb nanowire-Nb hybrid device, Nano Lett. **12**, 6414 (2012).

[21] J.-P. Xu, M.-X. Wang, Z. L. Liu, J.-F. Ge, X. Yang, C. Liu, Z. A. Xu, D. Guan, C. L. Gao, D. Qian *et al.*, Experimental Detection of a Majorana Mode in the Core of a Magnetic Vortex Inside a Topological Insulator-Superconductor $Bi_2Te_3/NbSe_2$ Heterostructure, Phys. Rev. Lett. **114**, 017001 (2015).

[22] S. Nadj-Perge, I. K. Drozdov, J. Li, H. Chen, S. Jeon, J. Seo, A. H. MacDonald, B. A. Bernevig, and A. Yazdani, Observation of Majorana fermions in ferromagnetic atomic chains on a superconductor, Science **346**, 602 (2014).

[23] H. Zhang, C.-X. Liu, S. Gazibegovic, D. Xu, J. A. Logan, G. Wang, N. Van Loo, J. D. S. Bommer, M. W. A. De Moor, D. Car *et al.*, Quantized Majorana conductance, Nature (London) **556**, 74 (2018).

[24] A. Das, Y. Ronen, Y. Most, Y. Oreg, M. Heiblum, and H. Shtrikman, Zero-bias peaks and splitting in an Al-InAs nanowire topological superconductor as a signature of Majorana fermions, Nat. Phys. **8**, 887 (2012).

[25] H.-H. Sun, K.-W. Zhang, L.-H. Hu, C. Li, G.-Y. Wang, H.-Y. Ma, Z.-A. Xu, C.-L. Gao, D.-D. Guan, Y.-Y. Li *et al.*, Majorana Zero Mode Detected with Spin Selective Andreev Reflection in the Vortex of a Topological Superconductor, Phys. Rev. Lett. **116**, 257003 (2016).

[26] Q. L. He, L. Pan, A. L. Stern, E. C. Burks, X. Che, G. Yin, J. Wang, B. Lian, Q. Zhou, E. S. Choi *et al.*, Chiral Majorana fermion modes in a quantum anomalous Hall insulator-superconductor structure, Science **357**, 294 (2017).

[27] M. Gong, S. Tewari, and C. Zhang, BCS-BEC Crossover and Topological Phase Transition in 3D Spin-Orbit Coupled Degenerate Fermi Gases, Phys. Rev. Lett. **107**, 195303 (2011).

[28] M. Gong, G. Chen, S. Jia, and C. Zhang, Searching for Majorana Fermions in 2D Spin-Orbit Coupled Fermi Superfluids at Finite Temperature, Phys. Rev. Lett. **109**, 105302 (2012).

[29] G. Chen, M. Gong, and C. Zhang, BCS-BEC crossover in spin-orbit-coupled two-dimensional fermi gases, Phys. Rev. A **85**, 013601 (2012).

[30] M. Iskin and A. L. Subaşı, Stability of Spin-Orbit Coupled Fermi Gases with Population Imbalance, Phys. Rev. Lett. **107**, 050402 (2011).

[31] W. Yi and G.-C. Guo, Phase separation in a polarized Fermi gas with spin-orbit coupling, Phys. Rev. A **84**, 031608(R) (2011).

[32] H. Hu, L. Jiang, X.-J. Liu, and H. Pu, Probing Anisotropic Superfluidity in Atomic Fermi Gases with Rashba Spin-Orbit Coupling, Phys. Rev. Lett. **107**, 195304 (2011).

[33] L. Jiang, X.-J. Liu, H. Hu, and H. Pu, Rashba spin-orbit-coupled atomic Fermi gases, Phys. Rev. A **84**, 063618 (2011).

[34] Z.-Q. Yu and H. Zhai, Spin-Orbit Coupled Fermi Gases Across a Feshbach Resonance, Phys. Rev. Lett. **107**, 195305 (2011).

[35] K. Zhou and Z. Zhang, Opposite Effect of Spin-Orbit Coupling on Condensation and Superfluidity, Phys. Rev. Lett. **108**, 025301 (2012).

[36] Z. Zheng, M. Gong, X. Zou, C. Zhang, and G. Guo, Route to observable Fulde-Ferrell-Larkin-Ovchinnikov phases in three-dimensional spin-orbit-coupled degenerate fermi gases, Phys. Rev. A **87**, 031602(R) (2013).

[37] L.-L. Wang, Q. Sun, W.-M. Liu, G. Juzeliūnas, and A.-C. Ji, Fulde-Ferrell-Larkin-Ovchinnikov state to topological superflu-

idity transition in bilayer spin-orbit-coupled degenerate Fermi gases, Phys. Rev. A **95**, 053628 (2017).

[38] L. He, H. Hu, and X.-J. Liu, Realizing Fulde-Ferrell Superfluids via a Dark-State Control of Feshbach Resonances, Phys. Rev. Lett. **120**, 045302 (2018).

[39] C. Qu, Z. Zheng, M. Gong, Y. Xu, L. Mao, X. Zou, G. Guo, and C. Zhang, Topological superfluids with finite-momentum pairing and Majorana fermions, Nat. Commun. **4**, 2710 (2013).

[40] W. Zhang and W. Yi, Topological Fulde-Ferrell-Larkin-Ovchinnikov states in spin-orbit-coupled Fermi gases, Nat. Commun. **4**, 2711 (2013).

[41] Z. Zheng, C. Qu, X. Zou, and C. Zhang, Floquet Fulde-Ferrell-Larkin-Ovchinnikov superfluids and Majorana fermions in a shaken fermionic optical lattice, Phys. Rev. A **91**, 063626 (2015).

[42] Z. Zheng, M. Gong, Y. Zhang, X. Zou, C. Zhang, and G. Guo, FFLO superfluids in 2D spin-orbit coupled fermi gases, Sci. Rep. **4**, 6535 (2014).

[43] E. M. Lifshitz and L. P. Pitaevskii, *Statistical Physics: Theory of the Condensed State* (Elsevier, Singapore, 2013), Vol. 9.

[44] R. K. Pathria and P. D. Beale, *Statistical Mechanics*, 3rd ed. (Elsevier/Academic Press, Amsterdam, Boston, 2011) .

[45] C. Kittel, *Introduction to Solid State Physics*, 8th ed. (Wiley, Hoboken, 2005) .

[46] S. R. Turns, *Thermodynamics: Concepts and Applications* (Cambridge University Press, New York, 2006).

[47] H. Guo, Y. He, C.-C. Chien, and K. Levin, Compressibility in strongly correlated superconductors and superfluids: From the BCS regime to Bose-Einstein condensates, Phys. Rev. A **88**, 043644 (2013).

[48] H.-Y. Wang, Z. Zheng, L. Zhuang, and W.-M. Liu, Topological supersolidity of dipolar fermi gases in a spin-dependent optical lattice, J. Phys.: Condens. Matter **32**, 235701 (2020).

[49] N. C. Costa, M. V. Araújo, J. P. Lima, T. Paiva, R. R. dos Santos, and R. T. Scalettar, Compressible ferrimagnetism in the depleted periodic Anderson model, Phys. Rev. B **97**, 085123 (2018).

[50] W. Zhang, S. Greschner, E. Fan, T. C. Scott, and Y. Zhang, Ground-state properties of the one-dimensional unconstrained pseudo-anyon Hubbard model, Phys. Rev. A **95**, 053614 (2017).

[51] P. M. Duarte, R. A. Hart, T.-L. Yang, X. Liu, T. Paiva, E. Khatami, R. T. Scalettar, N. Trivedi, and R. G. Hulet, Compressibility of a Fermionic Mott Insulator of Ultracold Atoms, Phys. Rev. Lett. **114**, 070403 (2015).

[52] V. I. Yukalov and R. Graham, Bose-Einstein condensed systems in random potentials, Phys. Rev. A **75**, 023619 (2007).

[53] Y.-R. Lee, M.-S. Heo, J.-H. Choi, T. T. Wang, C. A. Christensen, T. M. Rvachov, and W. Ketterle, Compressibility of an ultracold Fermi gas with repulsive interactions, Phys. Rev. A **85**, 063615 (2012).

[54] M. J. H. Ku, A. T. Sommer, L. W. Cheuk, and M. W. Zwierlein, Revealing the superfluid lambda transition in the universal thermodynamics of a unitary Fermi gas, Science **335**, 563 (2012).

[55] F. J. Poveda-Cuevas, P. C. M. Castilho, E. D. Mercado-Gutierrez, A. R. Fritsch, S. R. Muniz, E. Lucioni, G. Roati, and V. S. Bagnato, Isothermal compressibility determination across Bose-Einstein condensation, Phys. Rev. A **92**, 013638 (2015).

[56] P. C. M. Castilho, F. J. Poveda-Cuevas, J. A. Seman, R. F. Shiozaki, G. Roati, S. R. Muniz, D. V. Magalhaes, and V. S. Bagnato, Equation of state for a trapped quantum gas: Remnant of zero-point energy effects, New J. Phys. **18**, 023014 (2016).

[57] N. Gemelke, X. Zhang, C.-L. Hung, and C. Chin, In situ observation of incompressible Mott-insulating domains in ultracold atomic gases, Nature (London) **460**, 995 (2009).

[58] Let us define $g(x, y) = f(x, y, z)$, where $z = z(x, y)$, then $(\frac{\partial g}{\partial x})_y = (\frac{\partial f}{\partial x})_{y,z} + (\frac{\partial g}{\partial z})_{x,y}(\frac{\partial z}{\partial x})_y$. In the main text these two terms contribute to the explicit compressibility and implicit compressibility, respectively.

[59] W. Ketterle and M. W. Zwierlein, Making, probing and understanding ultracold fermi gases, arXiv:0801.2500.

[60] L. Han and C. A. R. Sá de Melo, Evolution from BCS to BEC superfluidity in the presence of spin-orbit coupling, Phys. Rev. A **85**, 011606(R) (2012).

[61] C. A. R. Sá de Melo, When fermions become bosons: Pairing in ultracold gases, Phys. Today **61**(10), 45 (2008).

[62] C. A. R. Sá de Melo, M. Randeria, and J. R. Engelbrecht, Crossover from BCS to Bose Superconductivity: Transition Temperature and Time-Dependent Ginzburg-Landau Theory, Phys. Rev. Lett. **71**, 3202 (1993).

[63] In degenerate gases with density $n \approx 1/\mu\text{m}^3$ and temperature $T \approx 10^{-6}$ K, the unit of pressure $1/\kappa_0 = \hbar^2(6\pi^2)^{2/3}n^{5/3}/(2m) \approx 5 \times 10^{-12}$ Pa for ^{7}Li.

[64] J. Zhou, W. Zhang, and W. Yi, Topological superfluid in a trapped two-dimensional polarized Fermi gas with spin-orbit coupling, Phys. Rev. A **84**, 063603 (2011).

[65] D. E. Sheehy and L. Radzihovsky, BEC-BCS crossover, phase transitions and phase separation in polarized resonantly-paired superfluids, Ann. Phys. (NY) **322**, 1790 (2007).

[66] K. S. Seo, C. Zhang, and S. Tewar, Thermodynamic signatures for topological phase transitions to Majorana and Weyl superfluids in ultracold Fermi gases, Phys. Rev. A **87**, 063618 (2013).

[67] N. Manini and L. Salasnich, Bulk and collective properties of a dilute fermi gas in the BCS-BEC crossover, Phys. Rev. A **71**, 033625 (2005).

[68] M. Cozzini and S. Stringari, Fermi Gases in Slowly Rotating Traps: Superfluid versus Collisional Hydrodynamics, Phys. Rev. Lett. **91**, 070401 (2003).

[69] G. D. Rosi and S. Stringari, Collective oscillations of a trapped quantum gas in low dimensions, Phys. Rev. A **92**, 053617 (2015).

[70] B. A. Gelman, E. V. Shuryak, and I. Zahed, Ultracold strongly coupled gas: A near-ideal liquid, Phys. Rev. A **72**, 043601 (2005).

[71] M. Bartenstein, A. Altmeyer, S. Riedl, S. Jochim, C. Chin, J. H. Denschlag, and R. Grimm, Collective Excitations of a Degenerate Gas at the BEC-BCS Crossover, Phys. Rev. Lett. **92**, 203201 (2004).

[72] M. Cozzini, S. Stringari, V. Bretin, P. Rosenbusch, and J. Dalibard, Scissors mode of a rotating Bose-Einstein condensate, Phys. Rev. A **67**, 021602(R) (2003).

[73] Z. Zheng, H. Pu, X. Zou, and G. Guo, Thermodynamic properties of Rashba spin-orbit-coupled Fermi gas, Phys. Rev. A **90**, 063623 (2014).